

CHAPTER V

PROGRAM VERIFICATION

The program developed by using C++ language can be used to solve the multicomponent and multistage distillation. The performance test of program is shown and is discussed in this chapter. Three methods for testing the reliability of the program are discussed below.

- Material balancing
- Comparison of the results to reference data sources
- Comparison of the results to a commercial simulator, i. e. HYSIM

Several study cases are tested. All of the outputs displayed on window are shown in Appendix A.

Case I (Henry, E. J., 1981)

Column configuration:

- 5 trays
- 1 feed
- no liquid and vapor sidestream
- no side exchanger

Feed condition:

- flowrate 45.8 kg mole/hr into tray 3.
- pressure 6.89 Bar
- temperature 324 K
- feed molar composition

n-butane	0.3
n-pentane	0.4
propane	0.3

Top product:

- no vapor top product
- liquid top product flowrate 22.5 kg mole/hr

Top pressure is 6.89 Bar

Bottom pressure is 6.89 Bar

The solution of this case is showed in detail in Appendix A.

The column in this case is a conventional distillation. The conventional distillation column is defined as one that has one feed and two product streams, i. e. the distillate and bottom products.

Case II (Henry, E. J., 1981)

Column configuration:

- 20 trays
- 2 feeds
- no liquid and vapor sidestream
- no side exchanger

Feed condition:

Feed 1:

- flowrate 349.6 kg mole/hr into tray 5.
- pressure 1.36 Bar
- temperature 366 K
- feed molar composition

n-heptane	0.00
-----------	------

phenol	0.99
toluene	0.01

Feed 2:

- flowrate 183.2 kg mole/hr into tray 12.
- pressure 1.36 Bar
- temperature 377 K
- feed molar composition

n-heptane	0.50
phenol	0.00
toluene	0.50

Top product:

- no vapor top product
- liquid top product flowrate 91.6 kg mole/hr

Top pressure is 1.36 Bar

Bottom pressure is 1.36 Bar

Case III (Shuzo Ohe, 2536)

Column configuration:

- 8 trays
- 1 feed
- no liquid and vapor sidestream
- no side exchanger

Feed condition:

- flowrate 100 kg mole/hr into tray 4.
- pressure 1.0 Bar
- temperature 380 K

- feed molar composition

benzene	0.50
ethylbenzene	0.25
p-xylene	0.25

Top product:

- no vapor top product
- liquid top product flowrate 52.1 kg mole/hr

Top pressure is 1.0 Bar

Bottom pressure is 1.0 Bar

Case IV (Shozo Ohe, 2536)

Column configuration:

- 9 trays
- 1 feed
- no liquid and vapor sidestream
- no side exchanger

Feed condition:

- flowrate 10.0 kg mole/hr into tray 6.
- pressure 10.1 Bar
- temperature 355 K
- feed molar composition

n-butane	0.25
n-hexane	0.25
n-pentane	0.25
propane	0.25

Top product:

- no vapor top product
- liquid top product flowrate 5.0 kg mole/hr

Top pressure is 10.1 Bar

Bottom pressure is 10.1 Bar

Case V (Henry, E. J., 1981)

Column configuration:

- 11 trays
- 1 feed
- no liquid and vapor sidestream
- no side exchanger

Feed condition:

- flowrate 45.36 kg mole/hr into tray 6.
- pressure 8.27 Bar
- temperature 355 K
- feed molar composition

2-methyl butane (i-pentane)	0.20
i-butane	0.15
n-butane	0.25
n-pentane	0.35
propane	0.05

Top product:

- no vapor top product
- liquid top product flowrate 22.18 kg mole/hr

Top pressure is 8.27 Bar

Bottom pressure is 8.27 Bar

The complex column which differs from a conventional distillation column is composed of more than one feed and/or more stream withdrawn in

addition to the distillate and bottom. The column in case V is modified as the complex column in the next case.

Case VI

The operating conditions are similar to case V except the product streams. This column has a liquid sidestream from stage 4 with flowrate 10 kg mole/hr. The liquid top product is changed to 12.18 kg mole/hr.

Case VII

The operating conditions are similar to case V except the product streams. The vapor sidestream is defined with flowrate 10 kg mole/hr from stage 3.

Case VIII

It has the same operating condition to case V. There is the cooling exchanger at stage 3 with heat rate 10000 J/hr.

5.1 Material Balancing

The distillation model shown in chapter III has been used to test the results of the simulation. The calculation procedure is the iterative method. The result are calculated from each equilibrium state. The summation of liquid and vapor composition on each tray must be equal to 1. Thus, the material balances are suitable to calculate the error from the output of program.

The component balances on each stage are shown in equation (5-1).

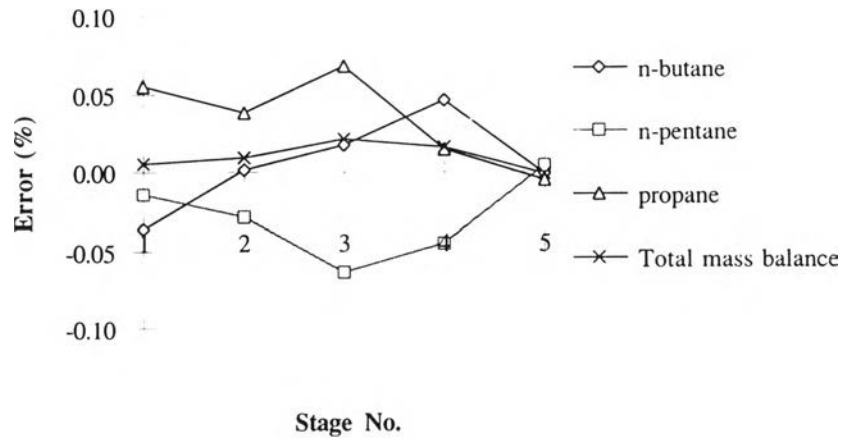
$$L_{j-1} x_{i,j-1} + V_{j+1} y_{i,j+1} + F_j z_{i,j} - (L_j + U_j) x_{i,j} - (V_j + W_j) y_{i,j} = E_{i,j} \quad (5-1)$$

where $E_{i,j}$ is the error of component i on stage j .

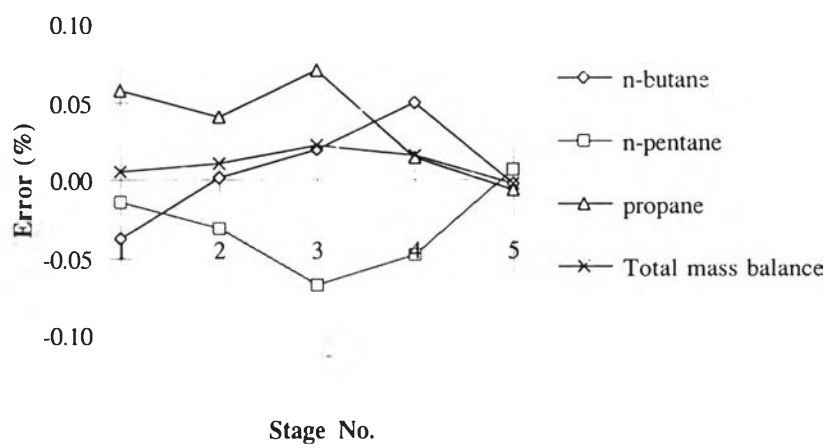
The overall material balances for each component around the column is expressed as the equation (5-2)

$$F_j z_{i,j} - \sum_{j=1}^N W_j y_{i,j} + \sum_{j=1}^N U_j x_{i,j} + V_1 y_{i,1} + L_N x_{i,N} = E_{\text{overall}} \quad (5-2)$$

This program provides several tables of simulation results as shown in appendix A. The subscript "DIST" shown in table refers to the results calculated by this simulator. It is convenient to show the errors of calculations by using graphs. The horizontal axis is the stage number and the vertical axis is the error of the results calculated by material balance confirmation.

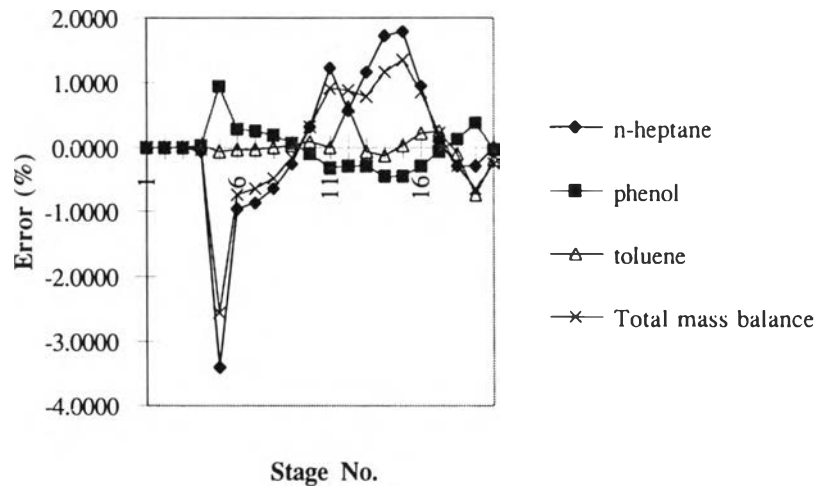


a) The result estimated by using Peng-Robinson (PR) correlation.

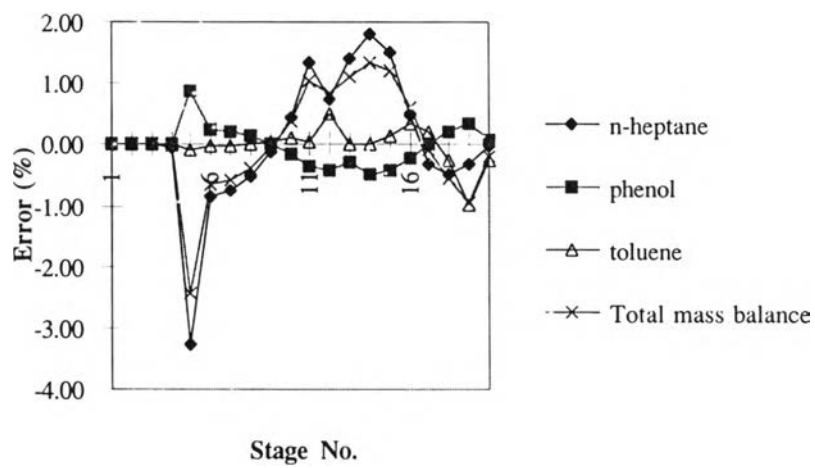


b) The result estimated by using Soave Redlich Kwong (SRK) correlation.

Figure 5.1 The error of material balance equation for case I.

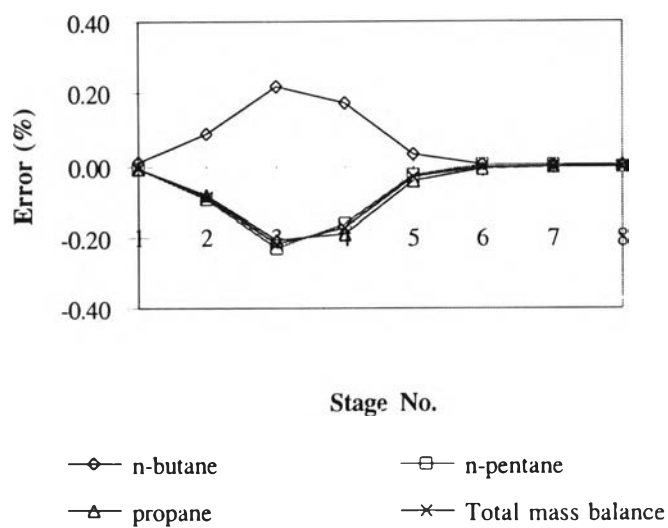


a) The result estimated by using Peng-Robinson (PR) correlation

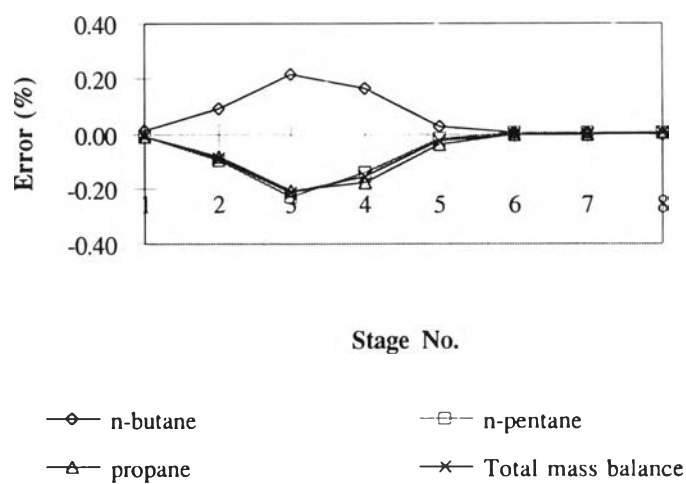


b) The result estimated by using Soave Redlich Kwong (SRK) correlation.

Figure 5.2 The error of material balance equation for case II.

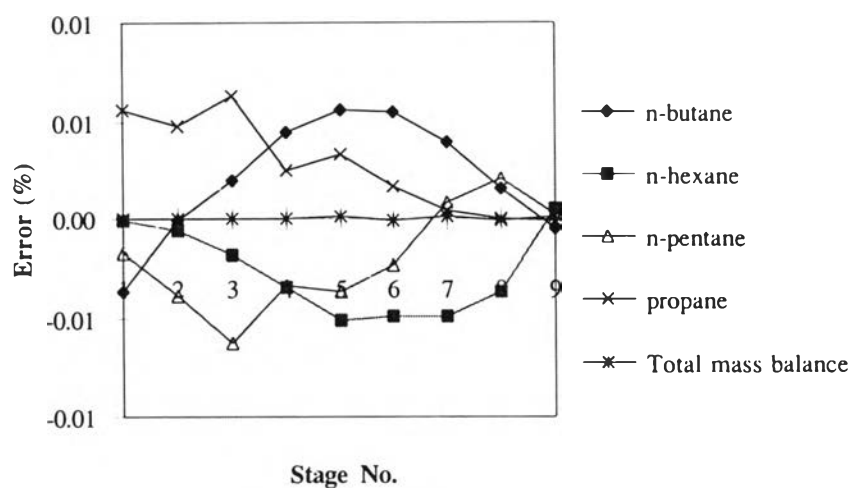


a) The result estimated by using Peng-Robinson (PR) correlation

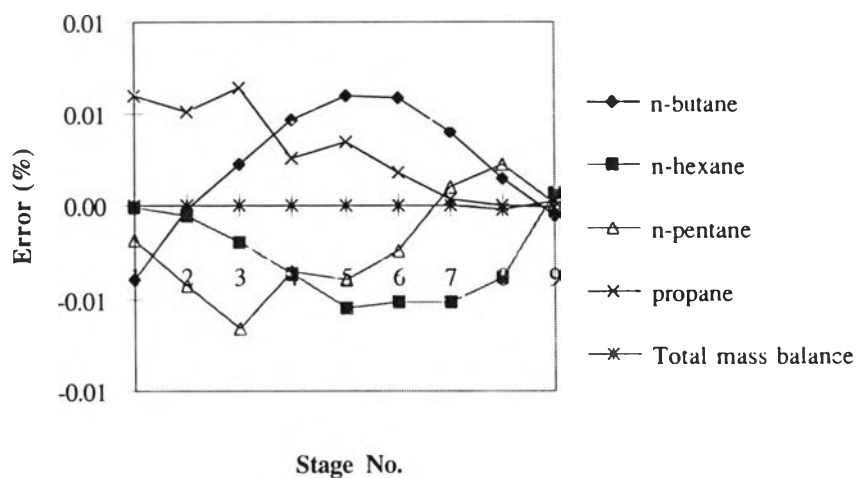


b) The result estimated by using Soave Redlich Kwong (SRK) correlation.

Figure 5.3 The error of material balance equation for case III.

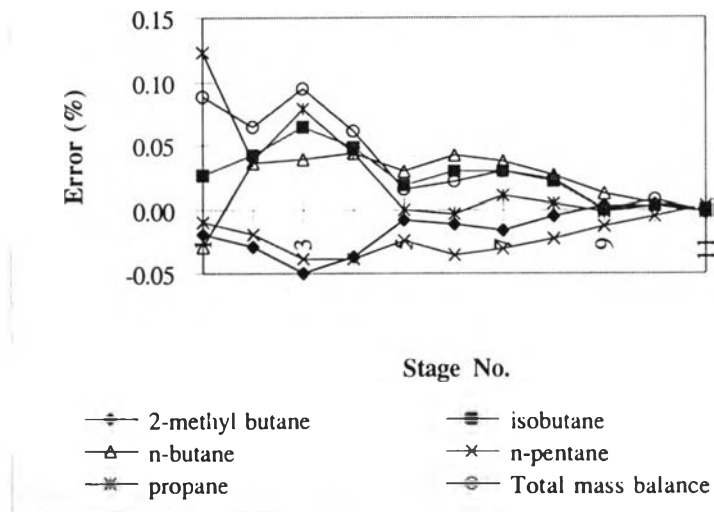


a) The result estimated by using Peng-Robinson (PR) correlation

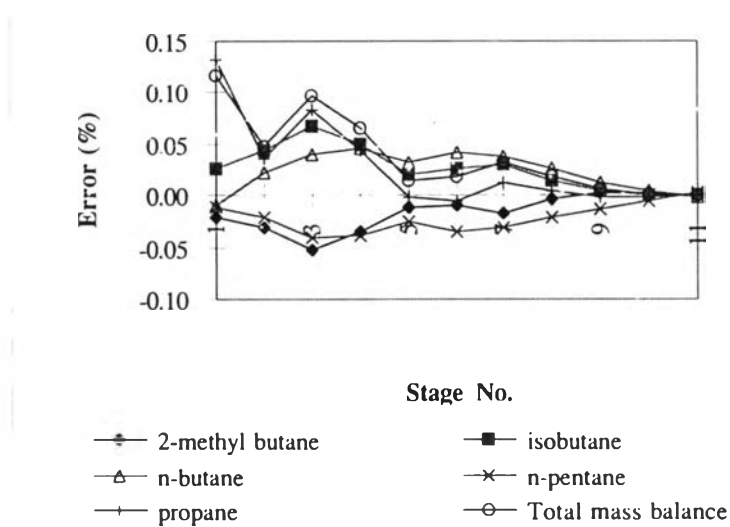


b) The result estimated by using Soave Redlich Kwong (SRK) correlation.

Figure 5.4 The error of material balance equation for case IV.



a) The result estimated by using Peng-Robinson (PR) correlation



b) The result estimated by using Soave Redlich Kwong (SRK) correlation.

Figure 5.5 The error of material balance equation for case V.

Considering figure 5.1, material balance errors of each component displays both over and under estimation in each tray. The total material balance errors in each tray are less than the components balance error. The total material balances using the PR model (to estimate the thermodynamic properties) has the error of 0.000005%. The maximum error for this case is -0.0117% presented in n-pentane balance. The results of case I using the PR model to estimate the thermodynamic properties has $\pm 0.0117\%$ as the maximum error.

For case I using the SRK model, the maximum error of $\pm 0.0601\%$ occurs in the total material balance. Figure 5.1 a) and b) have the same profiles. The error in condenser (stage 1) and reboiler (stage 5) are less than the errors shown in each stage of the column. The error in the column may be taken place by the energy balance equation used to determinate vapor and liquid interstage.

The error of case II shown in figure 5.2 a) has the same profile as figure 5.2 b). The error of each stage in column is comparatively higher than those of the condenser (stage 1) and reboiler (stage 20). The maximum error of the results using the PR model is $\pm 3.3936\%$. For the error of the results using the SRK model, $\pm 3.2567\%$ is the maximum value. The error of this case may be produced by poor estimation of phenol properties by using both modules.

The material balance relative errors of case III shown in figure 5.3 a) and b) have same distribution. The error in this case occurs in rectifying section, which is all stage above the feed tray. The maximum error of the results using the PR model is $\pm 0.2206\%$ and in case III using the SRK model, $\pm 0.2304\%$ is the maximum value.

Considering figure 5.4 and 5.5, the distribution of the material balance relative error in case IV has the same shape as case V. For case VI, VII and VIII the error distribution has the same as that of case V as shown in appendix A.

According to the results previously shown has the different error at each stage is observed, but the total material balance in that stage shows the

difference closed to zero. The maximum difference of each case is shown in table 5.1.

Table 5.1 Summary of the maximum material balance relative error.

Case	Maximum error	
	PR	SRK
I	0.0460	0.0497
II	-3.3936	-3.2567
III	0.2206	-0.2304
IV	-0.0063	-0.0066
V	0.1225	0.1330
VI	0.0480	0.0500
VII	0.0519	0.0557
VIII	0.1260	0.1330

The maximum difference is -3.3936% and -3.2667% of feed flowrate occurred in case II. Because the components in this case are the polar compounds, the equations of state available in this simulator can provide moderate accurate results for the polar compounds. (Thanit Sawasdisevi, 1996)

5.2 Comparison of the result to reference data sources

The reference has the result of calculation from Tridiagonal matrix method. The output calculated by the simulator have been compared to the temperature and liquid composition profile from the reference sources.

The results based on the different thermodynamic models, i. e. ideal gas, SRK, and PR are compared to the results of Tridiagonal matrix method.

Table 5.2 Comparison of temperature profiles of case III to the reference data.

Stage No.	Temperature (K)			Error (%)	
	PR_DIST	SRK_DIST	TDM_Ref	PR	SRK
1	354.21	354.59	-	-	-
2	359.58	360.04	359.48	-0.03	-0.16
3	372.05	372.74	372.26	0.06	-0.13
4	386.10	386.81	387.57	0.38	0.20
5	399.34	399.92	401.17	0.46	0.31
6	406.16	406.52	407.46	0.32	0.23
7	408.73	408.97	409.56	0.20	0.14
8	409.59	409.78	410.2	0.15	0.10

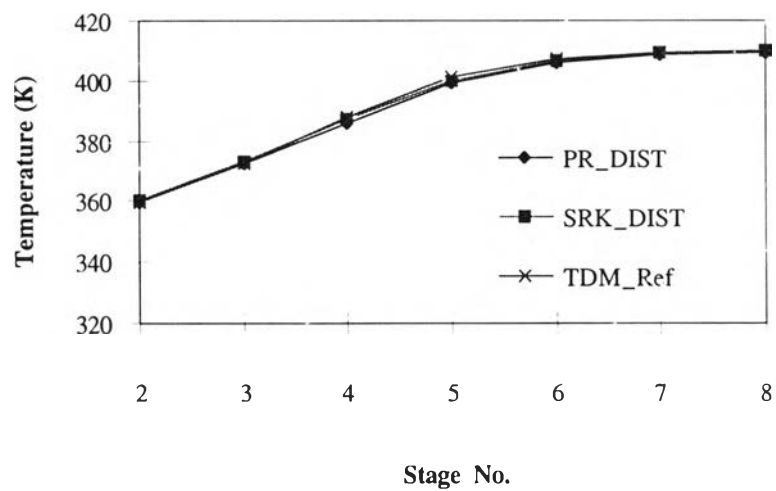


Figure 5.6 Temperature profile of case III.

Table 5.3 Comparison of liquid compositions of benzene to the reference data.

Stage No.	Liquid composition			Error (%)	
	PR_DIST	SRK_DIST	TDM_Ref	PR	SRK
1	0.951903	0.952214	0.958060	0.6427	0.6139
2	0.782865	0.779879	0.793870	1.3862	1.7940
3	0.483915	0.476467	0.481510	-0.4995	1.0584
4	0.253359	0.247296	0.232660	-8.8967	-5.9184
5	0.097505	0.093813	0.080040	-21.8203	-14.6813
6	0.032416	0.030862	0.023840	-35.9732	-22.7529
7	0.010083	0.009522	0.006710	-50.2683	-29.5316
8	0.002951	0.002768	0.001800	-63.9444	-34.9711

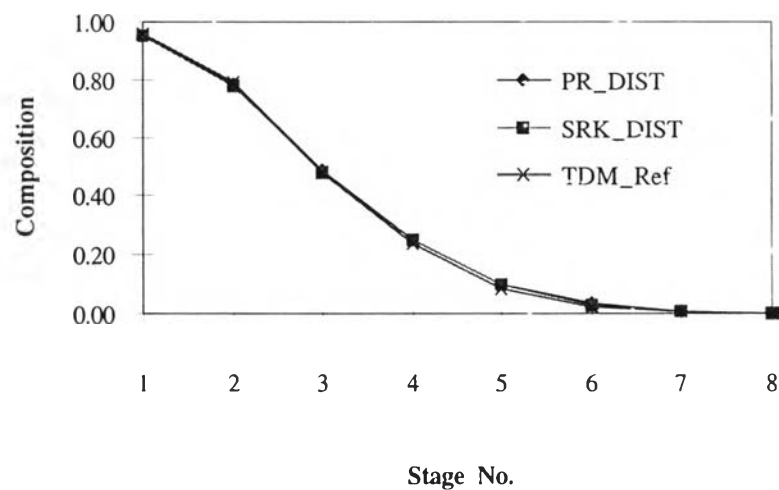


Figure 5.7 Liquid composition of benzene (Case III)

Table 5.4 Comparison of liquid compositions of ethylbenzene to the reference data

Stage No.	Liquid composition			Error (%)	
	PR_DIST	SRK_DIST	TDM_Ref	PR	SRK
1	0.027649	0.027525	0.024210	-14.2049	-12.0436
2	0.120841	0.122662	0.115500	-4.6242	-5.8388
3	0.278935	0.283214	0.282530	1.2724	-0.2415
4	0.392453	0.395892	0.406630	3.4865	2.7124
5	0.471167	0.473290	0.483450	2.5407	2.1467
6	0.498926	0.499852	0.505720	1.3434	1.1739
7	0.501888	0.502224	0.505010	0.6182	0.5547
8	0.494564	0.494623	0.495580	0.2050	0.1935

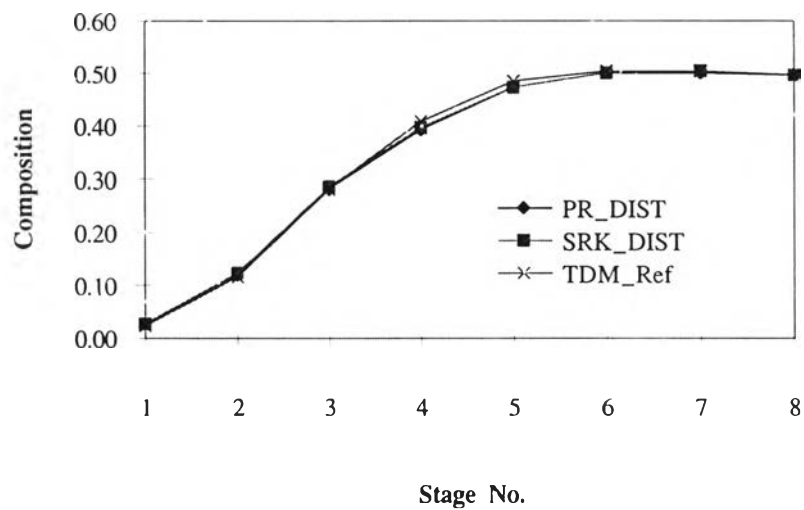


Figure 5.8 Liquid composition of ethylbenzene (Case III).

Table 5.5 Comparison of liquid compositions of toluene to the reference data

Stage No.	Liquid composition			Error (%)	
	PR_DIST	SRK_DIST	TDM_Ref	PR	SRK
1	0.020447	0.020261	0.017730	-15.3243	-12.4920
2	0.096294	0.097459	0.090630	-6.2496	-7.0070
3	0.237150	0.240319	0.235960	-0.5043	-1.8138
4	0.354188	0.356812	0.360710	1.8081	1.0925
5	0.431328	0.432897	0.436500	1.1849	0.8323
6	0.468658	0.469285	0.470440	0.3788	0.2461
7	0.488029	0.488254	0.488270	0.0494	0.0033
8	0.502485	0.502609	0.502620	0.0269	0.0022

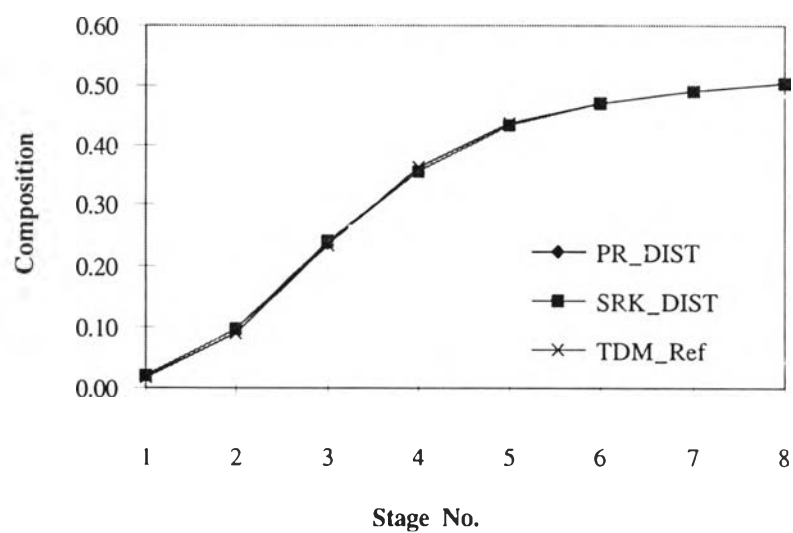


Figure 5.9 Liquid composition of toluene (Case III)

The temperature profiles calculated by this simulator and the reference data have the identical shape which are shown in figure 5.6. The results of simulator using different models to estimate the thermodynamic properties are compared to the reference data. The maximum relative error of each comparison is $\pm 0.46\%$ for the result using the PR model and $\pm 0.31\%$ for the SRK model.

Considering figure 5.7, all of the liquid compositions also has identical profiles. The composition in each stage has a small different value, but they have the large relative errors. For this case the liquid composition of benzene has poor estimation in stripping section, which is all stage below the feed tray including the feed tray itself. Because benzene, which is the light component, has low composition in stripping section such as 0.0018 of liquid flow from reboiler. Thus, the relative errors in rectifying section seem to be large. The relative error of liquid composition of benzene, $\pm 1.3362\%$ is the maximum value for the result using the PR model and $\pm 1.7940\%$ for the SRK model.

The liquid compositions of ethylbenzene and toluene shown in figure 5.8 and 5.9, respectively, have similar profile. Ethylbenzene and toluene are heavy components, which have low composition in rectifying section. Considering the stripping section, the maximum relative errors of ethylbenzene are $\pm 3.4865\%$ for the results using the PR model and $\pm 2.7124\%$ for the SRK model. For toluene, $\pm 1.8081\%$ is the maximum relative error of the results using the PR model and $\pm 1.0925\%$ is the maximum error which using the SRK model.

In this problem, the polar compound has thermodynamics properties which are estimated fairly by the equation of state. It is a part of the reason to produce the error. The difference from the SRK method is less than that of the PR method in this case.

5.3 Comparison of the results to a commercial simulator.

The results of the simulator are compared to those of a commercial simulator named HYSIM. HYSIM is commercially simulator available in department of chemical engineering, faculty of engineering, Chulalongkorn university. It is the process simulator designed for the gas processing, oil refining, petrochemical, chemicals, and synthetic fuels industries. (Hyprotech Ltd., 1991)

All of the results of each case compared to HYSIM are shown in appendix A. In this chapter, case I is used as the example to show the detail of comparison.

The output of this simulator displayed with the subscript DIST is shown in table and graphical form.

5.3.1 Comparison of temperature profiles

The results shown in table 5.6 are compared to HYSIM and the difference of each model presented as percentage of relative errors.

Table 5.6 Comparison of temperature profile for case I

Stage No.	Temperature (K)				Error (%)	
	PR_DIST	SRK_DIST	PR_HYSIM	SRK_HYSIM	PR	SRK
1	301.83	301.35	301.70	301.25	-0.04	-0.03
2	321.35	320.90	321.40	320.95	0.02	0.02
3	337.17	336.76	337.20	336.75	0.01	0.00
4	351.02	350.62	350.80	350.35	-0.06	-0.08
5	362.30	361.87	362.10	361.55	-0.06	-0.09

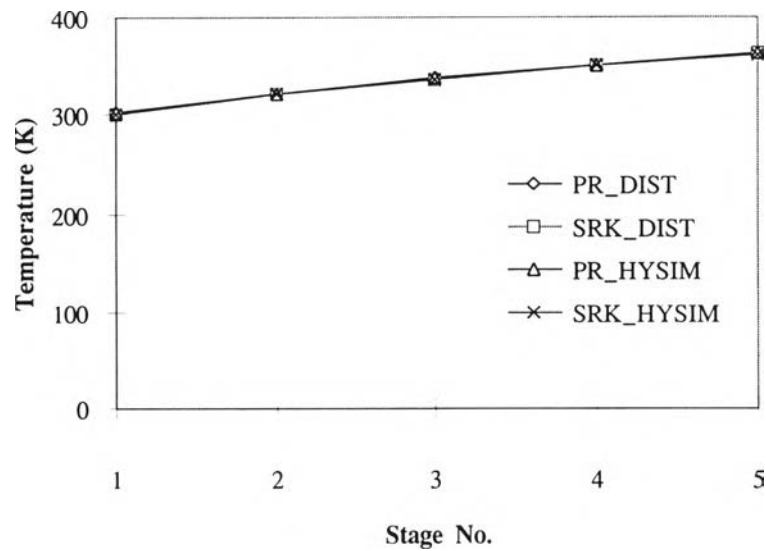


Figure 5.10 Temperature profiles of case I calculated by DIST and HYSIM.

Temperature of each case are plotted in the same axis as shown in figure 5.10. This figure shows the similar profiles. In this case, the maximum relative error of the results using the PR model is $\pm 0.06\%$. For the error from the result using the SRK model, $\pm 0.09\%$ is the maximum value.

The maximum relative errors of each case are shown in table 5.7. The details of each case are shown in appendix A.

Table 5.7 Summary of the maximum relative errors of temperature compared to HYSIM.

Case	Maximum error (%)	
	PR	SRK
I	-0.06	-0.09
II	0.42	0.41
IV	1.17	1.19
V	0.16	0.11
VI	0.06	0.10
VII	0.04	0.10
VIII	±0.05	0.10

5.3.2 Comparison of vapor composition profiles to HYSIM

The results and relative errors of vapor composition of n-butane, n-pentane and propane are shown in table 5.7, 5.8 and 5.9, respectively.

Table 5.8 Comparison of vapor compositions of n-butane to HYSIM (Case I)

Stage No.	Vapor composition of n-butane				Error (%)	
	PR_DIST	SRK_DIST	PR_HYSIM	SRK_HYSIM	PR	SRK
1	0.157493	0.156113	0.155673	0.154369	-1.1691	-1.1298
2	0.347837	0.348842	0.345682	0.346226	-0.6234	-0.7556
3	0.431815	0.434189	0.429248	0.430687	-0.5980	-0.8131
4	0.482633	0.485111	0.483394	0.485025	0.1574	-0.0177
5	0.405128	0.405765	0.408358	0.408968	0.7910	0.7832

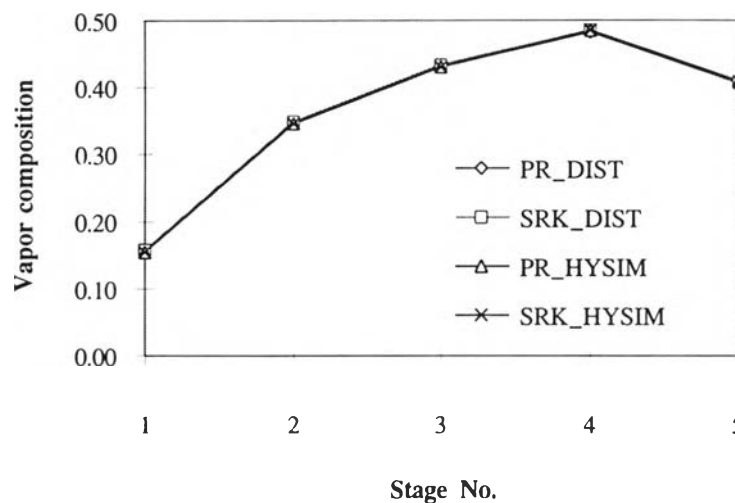


Figure 5.11 Vapor composition profiles of n-butane on case I.

The results plotted in figure 5.11 have the similar shape. The errors of rectifying section are comparatively high because n-butane which is the heavy component in this problem has low composition in that section.

Table 5.9 Comparison of vapor composition of n-pentane to HYSIM (Case I)

Stage No.	Vapor composition of n-pentane				Error (%)	
	PR_DIST	SRK_DIST	PR_HYSIM	SRK_HYSIM	PR	SRK
1	0.009552	0.009055	0.009813	0.009449	2.6597	4.1698
2	0.063283	0.061781	0.064485	0.063552	1.8640	2.7867
3	0.174184	0.172613	0.176029	0.175331	1.0481	1.5502
4	0.324037	0.323444	0.321459	0.321076	-0.8020	-0.7375
5	0.520432	0.521117	0.516604	0.516831	-0.7410	-0.8293

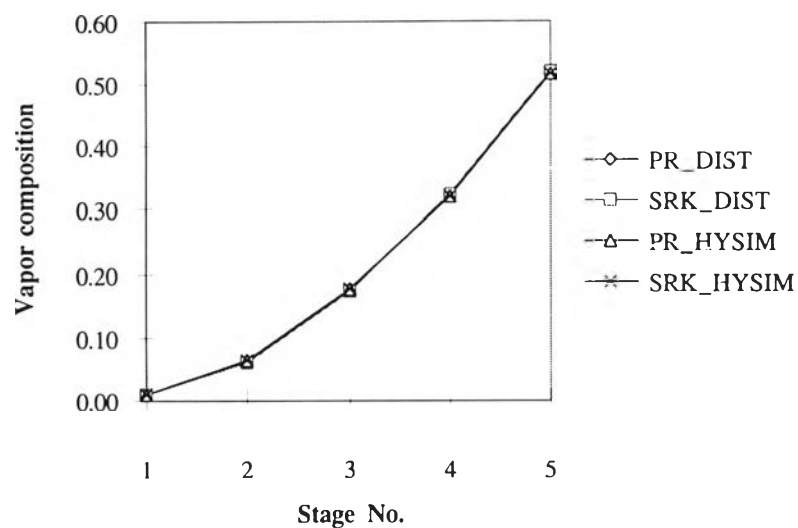


Figure 5.12 Vapor composition profiles of n-pentane on case I.

The results plotted in figure 5.12 have the similar shape. The errors of the rectifying section are high value which is the same as n-butane.

Table 5.10 Comparison of vapor compositions of propane to HYSIM (Case I)

Stage No.	Vapor composition of propane				Error (%)	
	PR_DIST	SRK_DIST	PR_HYSIM	SRK_HYSIM	PR	SRK
1	0.832955	0.834832	0.834513	0.836182	0.1867	0.1614
2	0.588880	0.589377	0.589832	0.590222	0.1614	0.1432
3	0.394001	0.393198	0.394722	0.393981	0.1827	0.1987
4	0.193330	0.191445	0.195147	0.193899	0.9311	1.2656
5	0.074440	0.073118	0.075038	0.074201	0.7969	1.4595

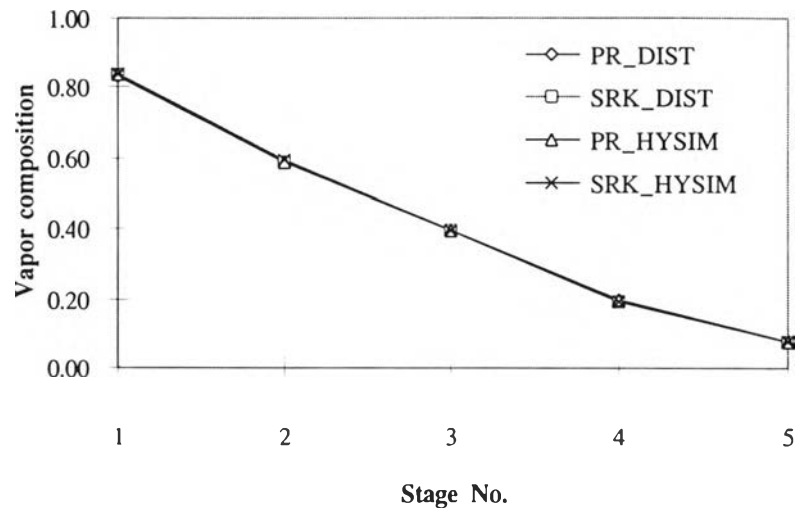


Figure 5.13 Vapor composition profiles of propane on case I.

Table 5.11 Summary of the maximum relative errors of vapor composition compared to HYSIM.

Case	Maximum error (%)	
	PR	SRK
I	2.6597	4.1698
II	44.4642	45.0026
IV	46.4706	47.5884
V	5.7377	14.5249
VI	3.4683	13.9520
VII	2.3065	12.5603
VIII	-4.2014	-14.5687

The maximum errors of each case are shown in table 5.11. The worst case is case II. The error may be produced by the poor estimation of polar

compound properties by the models used in this program. The best result using PR model is case VII. For the results using the SRK model with the minimum error is case I.

5.3.3 Comparison of liquid composition profiles to HYSIM

The results and relative errors of liquid composition of n-butane, n-pentane and propane are shown in table 5.12, 5.13 and 5.14, respectively.

Table 5.12 Comparison of liquid compositions of n-butane to HYSIM (Case I)

Stage No.	Liquid composition of n-butane				Error (%)	
	PR_DIST	SRK_DIST	PR_HYSIM	SRK_HYSIM	PR	SRK
1	0.347910	0.348919	0.345682	0.346226	-0.6445	-0.7778
2	0.477664	0.480735	0.475888	0.477794	-0.3732	-0.6155
3	0.423895	0.425563	0.421495	0.422179	-0.5694	-0.8016
4	0.365345	0.365587	0.367161	0.367263	0.4946	0.4563
5	0.253570	0.252584	0.255881	0.255363	0.9032	1.0883

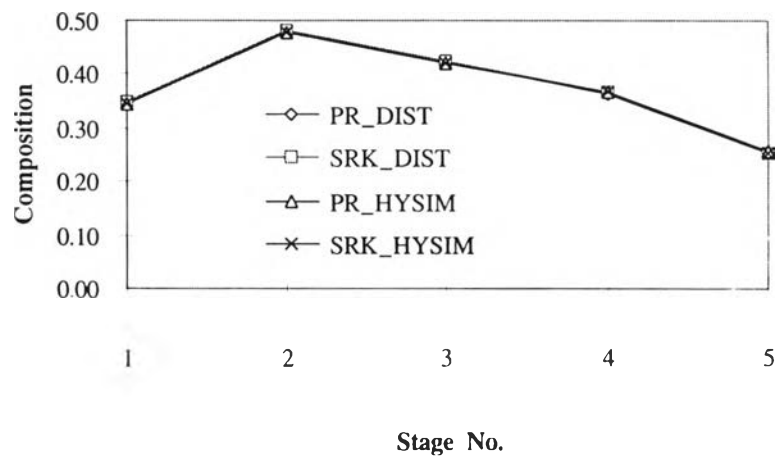


Figure 5.14 Liquid composition profiles of n-butane on case I.

Table 5.13 Comparison of liquid compositions of n-pentane to HYSIM (Case I)

Stage No.	Liquid composition of n-pentane				Error (%)	
	PR_DIST	SRK_DIST	PR_HYSIM	SRK_HYSIM	PR	SRK
1	0.063321	0.061820	0.064485	0.063552	1.8051	2.7253
2	0.234803	0.233133	0.238284	0.237675	1.4609	1.9110
3	0.427221	0.427033	0.430986	0.431578	0.8736	1.0531
4	0.574473	0.575333	0.572648	0.573321	-0.3187	-0.3509
5	0.726281	0.727788	0.724032	0.724890	-0.3106	-0.3998

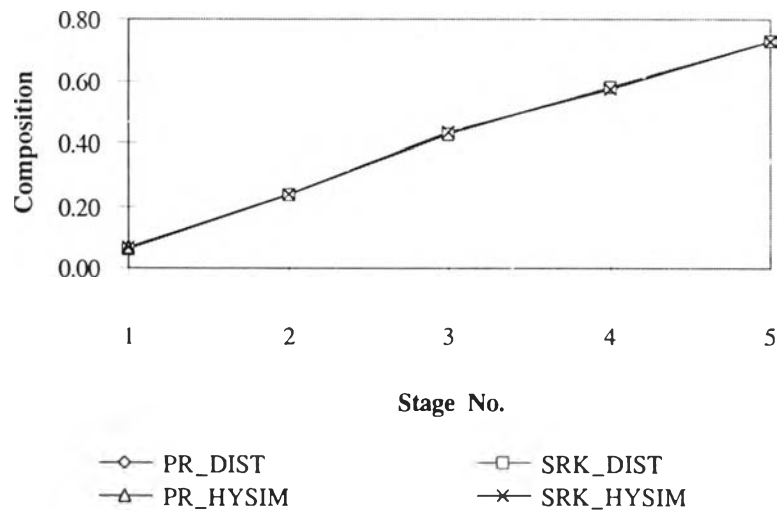


Figure 5.15 Liquid composition profiles of n-pentane on case I.

The results plotted in figure 5.14 have the similar shape. The errors of the rectifying section are relatively high because n-butane which is the heavy component in this problem has low composition in that section. Similarly,

the errors of n-pentane are high in rectifying section as shown in table 5.13. The liquid composition profiles have identical shapes shown in figure 5.15.

Table 5.14 Comparison of liquid compositions of propane to HYSIM (Case I)

Stage No.	Liquid composition of propane				Error (%)	
	PR_DIST	SRK_DIST	PR_HYSIM	SRK_HYSIM	PR	SRK
1	0.588769	0.58926	0.589832	0.590222	0.1802	0.1630
2	0.287533	0.286132	0.285828	0.284531	-0.5965	-0.5627
3	0.148884	0.147404	0.147519	0.146243	-0.9253	-0.7939
4	0.060182	0.05908	0.060191	0.059416	0.0150	0.5655
5	0.020149	0.019628	0.020087	0.019748	-0.3087	0.6077

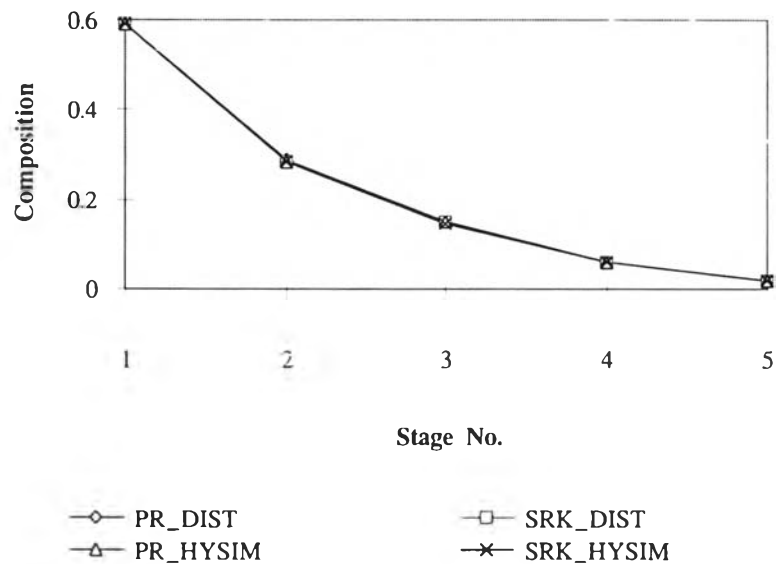


Figure 5.16 Liquid composition profiles of propane on case I.

The liquid composition profiles shown in figure 5.16 have similar shape. The high relative error occurs in stripping tray because propane which is the light component contain low composition in this section.

Table 5.15 Summary of the maximum relative error of liquid composition compared to HYSIM.

Case	Maximum error (%)	
	PR	SRK
I	1.8051	2.7253
II	45.0532	45.9584
IV	44.5151	45.6546
V	6.3492	10.6788
VI	3.0318	5.1742
VII	-9.5801	8.7373
VIII	-6.4516	-10.3448

The maximum error of each case are shown in table 5.15. The worst case is case II. The error may be produced by the poor properties estimation of polar compound by both modules. According to these data, the best result using PR model and SRK model are case I.

5.4 Sensitivity of simulator

This simulator allows users to change the tolerance (τ) in equations (3-30) and (3-31), as follows:

$$\tau = 0.01N \quad (5-3)$$

$$\tau = 0.001N \quad (5-4)$$

$$\tau = 0.0001N \quad (5-5)$$

where N is the number of stages.

The results of simulator which are different due to tolerance changed are checked by material balance of the column. The total material balance relative errors of case V are shown in table 5.16.

Table 5.16 The total material balance relative errors of case V.

Stage No.	Error (%)		
	0.01N	0.001N	0.0001N
1	0.0876	0.0349	0.0113
2	0.0648	0.0181	0.0062
3	0.0950	0.0098	0.0099
4	0.0613	0.0218	0.0034
5	0.0148	0.0068	0.0045
6	0.0210	0.0097	0.0108
7	0.0300	-0.0042	-0.0026
8	0.0237	0.0094	0.0019
9	-0.0004	0.0033	-0.0004
10	0.0064	0.0019	0.0038
11	-0.0026	-0.0013	-0.0021

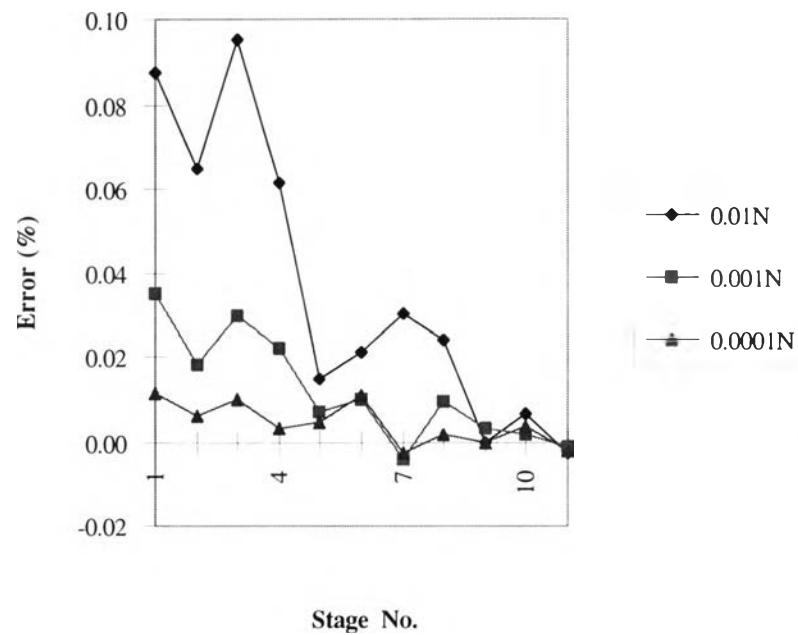


Figure 5.17 The total material balance relative errors of case V.

It is clearly seen from figure 5.17 that when the tolerance of 0.01N is used, it yields the maximum error. Whereas the tolerance of 0.001N and 0.0001N yield the errors of almost the same value. However it is seen that the tolerance of 0.0001N yields the minimum error. The maximum errors of 0.01N, 0.001N, and 0.0001N are 0.0613%, 0.0349% and 0.0113%, respectively.